Molecular Structure and Internal Rotation in 2,3,5,6-Tetrafluoroanisole as Studied by Gas-Phase Electron Diffraction and Quantum Chemical Calculations

Alexander V. Belyakov,[†] Martina Kieninger,[†] Raul E. Cachau,[‡] Oscar N. Ventura,[§] and Heinz Oberhammer*,[||]

St. Petersburg State Technological Institute, 190013, St. Petersburg, Russia; CCPG, Dequifim, Facultad de Química, Udelar, CC1157, 11800 Montevideo, Uruguay; Advanced Biomedical Computing Center, National Cancer Institute—Frederick, SAIC−Frederick Inc., Frederick 21702-1201, Maryland; and Institut für Physikalische und Theoretische Chemie, Universität Tübingen, 7207 Tübingen, Germany

Received: July 8, 2004; In Final Form: November 9, 2004

The geometric structure of 2,3,5,6-tetrafluoroanisole and the potential function for internal rotation around the C(sp^2)−O bond were determined by gas electron diffraction (GED) and quantum chemical calculations. Analysis of the GED intensities with a static model resulted in near-perpendicular orientation of the O−CH_3 bond relative to the benzene plane with a torsional angle around the C(sp^2)−O bond of τ(C−O) = 67(15)°. With a dynamic model, a wide single-minimum potential for internal rotation around the C(sp^2)−O bond with perpendicular orientation of the methoxy group [τ(C−O) = 90°] and a barrier of 2.7 ± 1.6 kcal/mol at planar orientation [τ(C−O) = 0°] was derived. Calculated potential functions depend strongly on the computational method (HF, MP2, or B3LYP) and converge adequately only if large basis sets are used. The electronic energy curves show internal structure, with local minima appearing because of the interplay between electron delocalization, changes in the hybridization around the oxygen atom, and the attraction between the positively polarized hydrogen atoms in the methyl group and the fluorine atom at the ortho position. The internal structure of the electronic energy curves mostly disappears if zero-point energies and thermal corrections are added. The calculated free energy barrier at 298 K is 2.0 ± 1.0 kcal/mol, in good agreement with the experimental determination.

Introduction

Fluorination has a strong effect on conjugation between oxygen lone pairs and adjacent π-bonds. Methyl vinyl ether, $CH_3OC(H)=CH_2$, possesses a low-energy planar syn conformation (CH_3−O bond is synperiplanar to C=C bond) and a high-energy nearly planar anti conformation.[1−3] Strong conjugation between the *p*-shaped lone pair at oxygen and the π(C=C) bond [n_π(O) → π^*(C=C)] leads to the preference of these sterically unfavorable structures. Fluorination of the vinyl group, $CH_3OC(F)=CF_2$, and perfluorination, $CF_3OC(F)=CF_2$, have a strong effect on the conformational properties. In these compounds the O−CH_3 and O−CF_3 bonds are nearly perpendicular to the plane of the vinyl group,[4] indicating that conjugation with the π-system is reduced. This may be attributed to anomeric effects, i.e., delocalization of the lone pair of the oxygen atom into the antibonding orbital of the adjacent C−F bond [n_π(O) → σ^*(C−F)].

Similarly, conjugation in anisole, $CH_3OC_6H_5$, stabilizes a planer structure.[5−7] Fluorination of the methyl group results in perpendicular orientation of the O−CF_3 bond in $CF_3OC_6H_5$ molecule.[8,9] In the current joint project between the electron diffraction laboratories at the Universities of Moscow, Ivanovo, and Tübingen; the St. Petersburg Technological Institute; and the computational chemistry group at the University of Montevideo, the effects of partial fluorination of the benzene ring on the conformational properties of anisole are investigated. Fluorination in the para position (4-fluoroanisole) and in para and meta positions (3,4-difluoroanisole) has no effect on the conformational properties.[10] Both compounds possess planar structures, as does the parent anisole. Fluorination in the ortho position (2-fluoroanisole) results in a mixture of 70(12)% planar conformer with τ[C(sp^2)−O] = 180° (methoxy group is opposite to fluorine atom) and 30(12)% nonplanar conformer with τ[C(sp^2)−O] = 58(8)°.[11]

In the present study, we report the results of a gas-phase electron diffraction study (GED) combined with quantum chemical calculations of 2,3,5,6-tetrafluoroanisole. Vibrational spectra (infrared and Raman) and a normal coordinate analysis do not provide any information about the conformation of the compound.[12] From long-range NMR coupling constants it was concluded that rotation around the C(sp^2)−O bond is nearly free with a slight preference for perpendicular orientation [τ(C−O) = 90°].[13] NMR data obtained in nematic phases do not allow a distinction between a 2-fold potential for internal rotation with a very low barrier and a 4-fold potential with a high barrier. In both cases the minima occur for planar structures.[14,15]

Quantum Chemical Calculations

The geometric parameters of tetrafluoroanisol were optimized for different fixed torsional angles τ(C−O), using initially the MP2(FC)/6-31G* theoretical model. This calculation resulted in a double-minimum potential energy curve, with a nearly perpendicular orientation of the O−CH_3 group with respect to

* Corresponding author. E-mail: heinz.oberhammer@uni-tuebingen.de.
[†] St. Petersburg State Technological Institute.
[‡] SAIC-Frederick Inc.
[§] CCPG.
[||] Universität Tübingen.

10.1021/jp046975d CCC: $30.25
Published on Web 12/24/2004

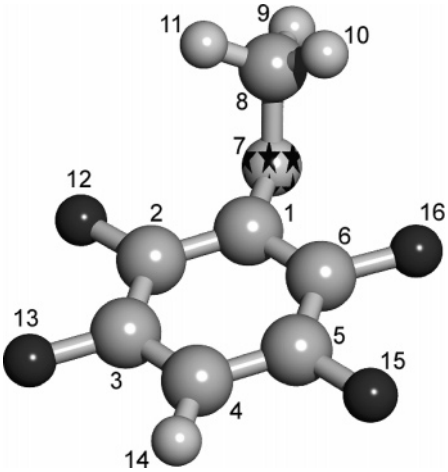

Figure 1. Molecular model with atom numbering.

the ring. Two such minima were located, at $\tau = 78.5°$ and 101.5°, separated by a small hump of only 0.10 kcal/mol at $\tau = 90°$. This small hump disappears, if zero-point energies are added to the electronic energies. The potential for internal rotation calculated at this level has a barrier of 0.68 kcal/mol at planar orientation ($\tau = 0°$). Additional calculations were performed, using different methods and larger basis sets, analogously to what was reported previously for *p*-fluoro-(trifluoromethoxy)benzene and related compounds[16] Besides the results, which were obtained at the MP2(Full)/6-311++G-(3df,2pd)[17−19] and B3LYP/pc-2[20,21] levels, the results at the HF/6-311++G(3df,2pd) will be also quoted for comparison purposes. Notice that the 6-311++G(3df,2pd) calculations involved 528 contracted and 768 primitive basis functions of spdf-type, while the smaller pc-2 calculations involved 416 contracted and 744 primitive basis functions of spdf-type. The reason to use the pc basis sets is that they were developed especifically to be used with DFT methods, while Pople basis sets were developed initially for working with molecular orbital methods. A 5° step was chosen for scanning the torsional angle between 0° and 90°. The rest of the geometrical parameters were optimized for each angle, to a precision of 10^{-3} Å in distances and 0.1° in angles. Calculations were performed in an SGI Altix using up to eight 1500 MHz Itanium2 processors, up to 8GB RAM and 70 GB storage space for the read−write file. The calculations were performed using the G03 program, revision B.04.[22] The results obtained at these levels of theory will be discussed later.

Structure Analysis

A molecular model with atom numbering is shown in Figure 1. In the structural analyses with static and dynamic models, the following assumptions were made. The C_6HF_4 group possess C_{2v} symmetry. All C−H bonds in the methyl group are equal. According to the calculations, the C(sp^2)−O bond is bent out of the phenyl plane by 2.5° in the perpendicular conformation, resulting in a C(3)−C(2)−C(1)−O angle of 177.5°. Theoretical data indicate that the C(2)−C(1)−O and C(1)−O−C(8) angles increase by 8.4 and 8.8°, respectively, when going from the perpendicular to the planar conformation. Variations of these angles where taken into account in the dynamic model. Differences between C−C bond lengths, between C−H bond lengths in the phenyl and methyl groups, and between C−C−C and C−C−F angles were fixed to calculated values (see Table 1). Furthermore, O−C−H angles; the out-of-plane angle of the C(sp^2)−O bond, C(3)−C(2)−C(1)−O; and the dihedral angle, C(1)−O−C(8)−H(9), were not refined. Vibrational amplitudes were collected in three groups: for bonded distances, nonbonded torsion-independent distances, and nonbonded torsion-dependent distances. The differences between the amplitudes in each group were fixed to calculated values. Amplitudes and vibrational corrections were derived from the MP2/6-31G* force field by the method of Sipachev,[23] which accounts for the nonlinear relation between Cartesian and internal coordinates. The inclusion of such corrections transforms r_a to r_{h1} values. The conventional method for calculating vibrational corrections that is based on perpendicular vibrations is not adequate in the case of large amplitude motions.

A preliminary analysis of the molecular intensities (Figure 2) and radial distribution curve (Figure 3) revealed that a structure with perpendicular orientation ($\tau = 90°$) of the methoxy group is in better agreement with the experimental data than a planar structure ($\tau = 0°$). This preliminary molecular model was then refined by least-squares fitting of the molecular intensities, using a static molecular model. Least-squares refinements were carried out with a modified version of the program KCED25.[24] Weight matrixes were diagonal, the long distance data were assigned unit weight, and the short distance data weight was 0.5. Taking the above restrictions into account, 10 geometric parameters [five bond lengths, four bond angles, and the torsional angle τ(C−O)], three groups of vibrational amplitudes, and two scale factors were refined simultaneously. The following correlation coefficients had values larger than 0.70, where u_{ind} is the vibrational amplitude for the group of nonbonded distances that do not depend on internal rotation around C(sp^2)−O bond: [C−F/C(sp^2)−O] = 0.85, [C−F/u_{ind}] = 0.75, [∠C(2)−C(1)−C(6)/∠C(1)−C(2)−F(12)] = 0.77, [∠C(2)−C(1)−O/τ(C−O)] = 0.95. The agreement factor for the static model with an effective torsional angle τ(C−O) = 67(15)° was $R = 4.8\%$.

In the dynamic model,[25] the large amplitude torsional motion around the C(sp^2)−O bond was simulated by a mixture of 10 pseudoconformers with torsional angles between 0° and 90°, in steps of 10°. Each pseudoconformer was weighted with a Boltzmann distribution function given by eq 1

$$P(\tau) = N \exp(-V(\tau)/RT) \qquad (1)$$

where a potential function of the form

$$V(\tau) = \frac{1}{2} V_2(1 + \cos 2\tau) + \frac{1}{2} V_4(1 + \cos 4\tau) \qquad (2)$$

was used. This potential function possesses maxima for planar structures [τ(C−O) = 0° and 180°] and minima at perpendicular or near-perpendicular orientation of the O−CH_3 group, depending on the ratio V_4/V_2. The barrier to internal rotation between perpendicular and planar orientation is V_2. For the dynamic model the potential parameter V_2 was refined instead of the torsional angle τ(C−O). Vibrational amplitudes and corrections were calculated for each pseudoconformer, excluding contributions from the low-frequency torsional vibration around the C(sp^2)−O bond. Only two groups of vibrational amplitudes, for bonded distances and for nonbonded torsion-independent distances, were refined. Due to high correlations it was not possible to refine the parameter V_4 in the least squares analyses. Refinements were performed for fixed values of $V_4 = 0.0$, 0.5, 1.0, and 1.5 kcal/mol. Because of the strong correlation between V_2 and V_4, the agreement factor R depends little on V_4. The best fit of the experimental intensities with $R = 5.0\%$ was obtained for $V_4 = 0.5$ kcal/mol and $V_2 = 2.7(16)$ kcal/mol. This agreement factor is slightly higher than that for the rigid model

TABLE 1: Experimental Structural Parameters of 2,3,5,6-Tetrafluoroanisole (Bond Lengths r_a in Å, Bond Angles $\angle_\alpha$ in deg, Amplitudes u and Vibrational Corrections $r_{h1} - r_a$ in 10^{-3} Å) and Ab Initio Values [MP2/6-311++G(3df,2p) for Geometric Parameters and MP2/6-31G* for Vibrational Parameters][a]

	static model			dynamic model[d]		ab initio	
	r_a	u	$r_{h1} - r_a$	r_a	u	r_e	u
C(1)−C(2)	1.403(9)	47(4)	1	1.403(9)	46(4)	1.393	44
C(2)−C(3)[b]	1.395(9)	46(4)	1	1.395(9)	46(4)	1.385	44
C(3)−C(4)[b]	1.392(9)	46(4)	0	1.392(9)	46(4)	1.382	44
C−F_{av}	1.344(9)	45(4)	0	1.346(6)	45(4)	1.330	43
C(1)−O	1.358(34)	46(4)	0	1.347(29)	46(4)	1.353	44
C(8)−O	1.437(22)	51(4)	0	1.439(22)	50(4)	1.428	48
C−$H_{Me\,av}$	1.113(32)	77(4)	1	1.113(34)	77(4)	1.087	75
C−H_{Ph}[b]	1.104(32)	76(4)	2	1.104(34)	76(4)	1.078	74
C(2)−C(1)−C(6)	118.1(22)			117.5(18)		118.8	
C(3)−C(4)−C(5)[b]	117.5(22)			117.3(18)		118.2	
C(2)−C(1)−O	121.6(81)			121.2b		121.0	
C(1)−O−C(8)	116.6(32)			117.4(34)		112.7	
O−C(8)−$H(9)_{fix}$	106.2			106.2		106.2	
O−C(8)−H(10/11)[b]	110.5			110.5		110.5	
C(1)−C(2)−F(12)	119.7(17)			120.5(15)		119.6	
C(2)−C(3)−F(13)[b]	118.8(17)			119.5(15)		118.8	
τ[C(sp^2)−O]	67(15)			90.0		80.3	
C(1)−O−C(8)−$H(9)_{fix}$	179.8			180.0		179.8	
C(3)−C(2)−C(1)−O_{fix}	177.5			177.5		177.5	
F(12)···F(13)	2.699(23)	104(4)	9	2.698(17)	102(3)	2.686	100
F(13)···F(15)	4.716(25)	73(4)	15	4.696(15)	73(3)	4.696	69
F(12)···F(16)	4.735(33)	74(4)	17	4.758(28)	73(3)	4.702	70
F(12)···F(15)	5.439(12)	66(4)	22	5.404(11)	66(3)	5.424	62
F(16)···O	2.749(174)	106(4)	9	2.781(18)	99(3)	2.732	103
F(12)···O	2.775(171)	113(4)	7	2.781(18)	99(3)	2.745	110
F(15)···O	4.735(92)	79(4)	20	4.751(18)	75(3)	4.729	75
F(13)···O	4.752(109)	77(4)	17	4.751(18)	75(3)	4.751	74
F(13)···C(2)	2.353(8)	62(4)	4	2.366(5)	62(3)	2.340	58
F(13)···C(4)	2.361(13)	61(4)	5	2.352(8)	62(3)	2.344	58
F(12)···C(3)	2.364(13)	62(4)	7	2.354(10)	62(3)	2.346	58
F(12)···C(1)	2.372(16)	63(4)	5	2.384(14)	62(3)	2.350	59
F(15)···C(3)	3.606(11)	61(4)	10	3.597(7)	62(3)	3.596	58
F(16)···C(2)	3.626(21)	62(4)	13	3.632(17)	62(3)	3.611	58
F(13)···C(1)	3.634(19)	62(4)	12	3.646(17)	63(3)	3.618	59
F(12)···C(4)	3.641(10)	62(4)	11	3.636(8)	62(3)	3.618	59
F(15)···C(2)	4.101(7)	64(4)	15	4.101(7)	65(3)	4.098	61
F(16)···C(3)	4.101(7)	65(4)	15	4.100(7)	65(3)	4.095	61
C(6)···O	2.392(89)	66(4)	7	2.394(22)	62(3)	2.380	62
C(2)···O	2.407(115)	66(4)	5	2.394(22)	62(3)	2.390	62
C(5)···O	3.658(58)	64(4)	13	3.659(24)	63(3)	3.652	61
C(3)···O	3.668(79)	64(4)	12	3.659(24)	63(3)	3.672	61
C(4)···O	4.185(27)	67(4)	12	4.184(26)	67(3)	4.175	63
C(1)···C(8)	2.375(39)	74(4)	5	2.347(45)	71(3)	2.315	71
C(3)···C(5)	2.375	57(4)	7	2.372	58(3)	2.371	54
C(2)···C(6)	2.398(24)	57(4)	9	2.393(16)	58(3)	2.398	54
C(1)···C(3)	2.424(21)	57(4)	8	2.428(20)	58(3)	2.413	54
C(2)···C(4)	2.429(6)	57(4)	5	2.431(4)	58(3)	2.418	54
C(2)···C(5)	2.763(10)	63(4)	9	2.760(7)	64(3)	2.765	60
C(1)···C(4)	2.834(24)	65(4)	6	2.842(23)	65(3)	2.822	62
F(12)···C(8)	3.038(58)	180(33)	3	3.397(58)	109	3.152	219
F(16)···C(8)	3.677(68)	219(33)	54	3.397(58)	109	3.500	258
F(13)···C(8)	5.284(42)	123(33)	8	5.470(56)	114	5.290	162
F(15)···C(8)	5.671(69)	166(33)	44	5.470(56)	114	5.536	205
C(2)···C(8)	3.070(33)	87(33)	−1	3.221(56)	88	3.080	126
C(6)···C(8)	3.402(55)	133(33)	31	3.221(56)	88	3.264	172
C(3)···C(8)	4.363(41)	78(33)	6	4.456(57)	101	4.333	117
C(5)···C(8)	4.601(60)	120(33)	29	4.456(57)	101	4.491	160
C(4)···C(8)	5.021(53)	85(33)	16	4.992(59)	114	4.933	124
R-factor (%)		4.8		5.0			

[a] Parenthesized values are three times the standard deviations. [b] Dependent parameter. [c] Vibrational amplitudes were refined in three groups (static model) and two groups (dynamic model) for bonded, nonbonded distances independent and dependent on rotation. [d] $V_2 = 2.7(16)$ kcal·mol^{-1}, $V_4 = 0.5$ kcal·mol^{-1}, fixed.

(4.8%), since only two groups of vibrational amplitudes were refined for the dynamic model as compared to three groups for the static model. Values of $V_4 = 0.0$ and 0.5 kcal/mol lead to single-minimum potentials and values of $V_4 = 1.0$ and 1.5 kcal/mol lead to double-minimum potentials with a small hump at τ(C−O) = 90°. The uncertainty of V_4 is estimated to be ±0.5 kcal/mol. For increasing values of V_4 from 0.0 to 1.0 kcal/mol, the refined value for V_2 decreases from 3.0(16) to 1.7(16) kcal/mol. Thus, the barrier to internal rotation, which is given by V_2 is determined by the GED experiment to be 2.7 ± 1.6 kcal/

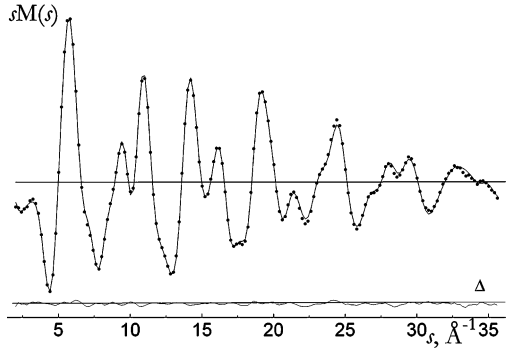

Figure 2. Experimental (dots) and calculated (full line) molecular intensities for dynamic model and residuals.

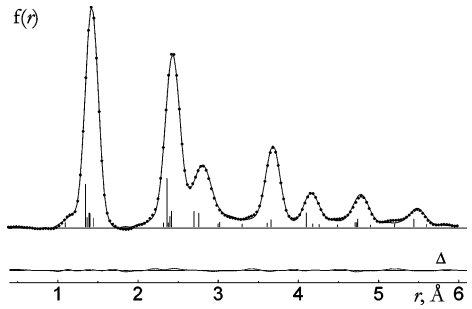

Figure 3. Experimental (dots) and calculated (full line) radial distribution curve for dynamic model and residuals.

mol. The GED experiment cannot discriminate between a single-minimum potential and a double-minimum potential with a small hump at τ(C−O) = 90°. A dynamic model with free internal rotation ($V_2 = V_4 = 0$) results in R = 5.6%. Considering that only a small portion of interatomic distances is affected by internal rotation, this increase implies a remarkably worse agreement. The following correlation coefficients had values larger than 0.70 in the least-squares analysis with a dynamic model: [C−F/C(sp^2)−O] = 0.85, [C−F/u_{ind}] = 0.75, [∠C(2)−C(1)−C(6)/∠C(1)−C(2)−F(12)] = 0.77.

Discussion

Geometric parameters and vibrational amplitudes obtained with the rigid and dynamic models are summarized in Table 1 together with calculated values [MP2(Full)/6-311++G(3df,2pd) values for geometric parameters and MP2/6-31G* values for vibrational amplitudes and corrections]. Estimated standard deviations calculated by the program were multiplied by a factor of 3 to include uncertainties due to data correlation and nonrefined vibrational amplitudes as well as a possible scale error of 0.1%. If a rigid model is used in the analysis, a structure with an "effective" torsional angle of τ(C−O) = 67(15)° is obtained. This result is compatible with the result obtained with a dynamic model for internal rotation around the C(sp^2)−O bond. This analysis results in a wide single-minimum potential with perpendicular orientation of the methoxy group relative to the phenyl plane [τ(C−O) = 90°] and a barrier to internal rotation of 2.7 ± 1.6 kcal/mol at τ(C−O) = 0°. The experimentally derived potential function is shown in Figure 4 together with theoretical curves.

Quantum chemical calculations result in curves with some fine structure that can clearly be correlated with physical phenomena. Hartree−Fock calculations do predict a minimum for the perpendicular conformation and a barrier of 1.4 kcal/mol, comparable to the experimental value if we consider its large uncertainty. The addition of correlation energy in post-

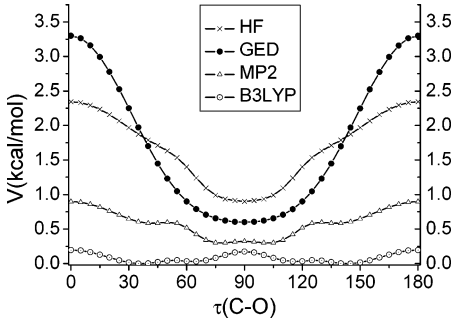

Figure 4. Experimental and calculated potential functions for internal rotation around the C(sp^2)−O bond. The experimental curve corresponds to a function given by eq 7 with V_2 = 2.7(16) kcal/mol and V_4 = 0.5 kcal/mol. The calculated functions were derived with 6-311++G-(3df,2pd) basis sets.[17] The individual curves are shifted by 0.3 kcal/mol.

Hartree−Fock MP2 calculations including all electrons produce several modifications. In the first place, the barrier is now much lower, about 0.6 kcal/mol smaller than the experimental barrier. Furthermore, a small hump is observed at τ = 90°, with two minima located symmetrically to both sides. There is a very small barrier of 0.02 kcal/mol separating these minima, and probably this feature is completely unimportant to determine the real minimum. It must be said that the hump is basis-set dependent and much smaller at the MP2/6-311++G(3df,2pd) level than at the MP2/6-31G* level. Finally, there is a shoulder at about 55° that corresponds to the conformation with the shortest F12···H11 distance, stabilized by electrostatic attraction. The density functional calculation at the B3LYP level predicts a very flat curve that in fact would correspond to almost barrierless internal rotation. This seems not to be the case, according to the experimental analysis, and one could then consider that the B3LYP description of this potential is definitely wrong. At any rate, the theoretical results are clearly compatible with a perpendicular structure with large amplitude vibrations along the internal rotation coordinate.

It was pointed out in the previous section that the experimental data can be best fit with a single-minimum potential energy curve, with a (V_2, V_4) pair of (2.7 ± 1.6, 0.5 ± 0.5) kcal/mol, although it was not possible to refine completely V_4. The calculated curves derived with the MP2 or B3LYP method discussed up to now do not agree with this description. However, there is no reason to expect so, since the theoretical curves show only the electronic energy plus the electrostatic interaction of the fixed nuclei and do not contain therefore any vibrational or rotational contributions. Moreover, the experiments were performed at room temperature. It would thus be necessary to compare the experimental curve with a calculated free-energy curve to obtain meaningful results. This could not be done in this work, but an approximation to the problem was devised. The first step was to analyze what happened when the zero-point energy (zpe) correction was calculated for each of the critical points. The raw and zpe-corrected energy values for the critical points are shown in Table 2 for the B3LYP and MP2(Full) calculations employing the pc-2 basis set, while a schematics of the arrangement of the critical points in each case is shown in Figure 5.

The conclusion is that the internal structure of the curves disappears almost completely after the correction. In the case of B3LYP, only a M0 minimum at the previous position of SP2 and saddle points at SP0 and SP1 remain, while at the MP2(Full) level, only the SP0 saddle point and the M0 minimum, at the previous position of SP1, remain. The MP2 curve is now

TABLE 2: Relative[a] Total Energies, Zpe-Corrected Energies, and Free Energies (all in kcal/mol) for the Critical Points on the Potential Energy Curves Calculated at the B3LYP/pc-2 and MP2(Full)/pc-2 Level

critical point[b]	B3LYP			MP2(Full)		
	$\Delta\Delta E^c$	$\Delta\Delta(E+\mathrm{ZPE})$	$\Delta\Delta G_{298}$	$\Delta\Delta E^c$	$\Delta\Delta(E+\mathrm{ZPE})$	$\Delta\Delta G_{298}$
SP0	0.00	0.00	0.00	0.00	0.00	0.00
M1	−0.20	−0.23		−0.34	−0.42	
SP2	−0.15	−0.32		−0.34	−0.50	
M0	−0.17	−0.30	−1.73	−0.58	−0.75	−2.01
SP1	−0.02	−0.25	−0.53	−0.53	−0.79	−1.05

[a] With respect to the energy of SP0. [b] The nomenclature for the critical points is derived from their nature and location on the potential energy curves: saddle points are identified as SP and minima as M; SP0 corresponds to the planar structure, while SP1 corresponds to the perpendicular structure; M0 is the minimum nearer to SP1, while M1 is the minimum nearer to SP0 and SP2 is the saddle point between both minima. [c] The total energy E is the electronic energy plus the classical electrostatic energy among the nuclei.

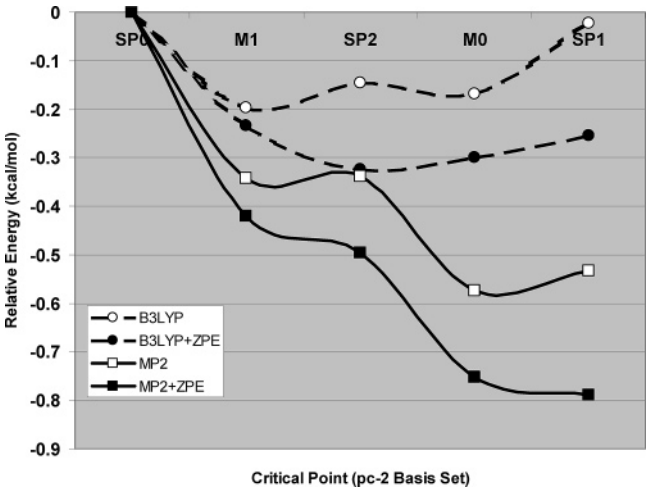

Figure 5. Comparison of the B3LYP/pc-2 and MP2(Full)/pc-2 curves with and without inclusion of the zero-point energy.

analogous to the experimental one, while in the B3LYP case the barrier at SP1 is quite low and in fact the picture is that of a wide amplitude vibration on a single minimum curve. This would be the situation observed in a low-temperature experiment. Since the experiments were performed at room temperature, a second step would be to compare the free energy values of the remaining critical points. Using SP0 as the reference, the M0 minimum free energy is obtained as −1.7 and −2.0 kcal/mol for the B3LYP and MP2 curves, respectively, the only remaining difference being that SP1 is higher for B3LYP than for MP2 (−0.5 kcal/mol at the B3LYP level vs −1.1 kcal/mol at the MP2 level). Thus, the effect of including the thermal corrections and the entropy into the calculations is to increase the barrier by about 1.7 kcal/mol in the B3LYP case and about 1.4 kcal/mol in the MP2 case. The values obtained now for the barrier are in much better agreement with the experimental one and within the error bars, with an estimated MP2(Full)/pc-2 value for the theoretical barrier at 298 K of 2.0 ± 1.0 kcal/mol. Nonetheless, this calculation is highly approximate and can only be taken as indicative of the true situation because of several flaws. In the first place, only harmonic frequencies were employed both for computing the zpe and $\Delta\Delta G_{298}$. In the second place, the internal rotation of the methyl group should have been taken into account in a rigorous vibrational analysis, instead of considering the corresponding degree of freedom as a vibration. Finally, an accurate treatment of the vibrational problem should consider the rotational coordinate θ as a "reaction coordinate", calculating the projected force constant matrix at each point on the path and performing the anharmonic and free-rotor corrections at each point on the path. This type of calculation is extremely demanding and, in our opinion, would not add substantially to the conclusion that indeed the theoretical and experimental pictures of the barrier for internal rotation in 2,3,5,6-tetrafluoroanisole are essentially in agreement. The calculation, however, may be valuable in connection to low-temperature studies of this barrier of rotation.

Experimental Section

A commercial sample of 2,3,5,6-tetrafluoroanisole with a purity of 97% was purchased from Aldrich. Before the GED experiment, part of the sample was pumped off in order to remove possible impurities with higher volatility. GED data were recorded with the KD-G2 unit at Tübingen with an accelerating voltage of about 60 kV.[26] The electron wavelength was calibrated against ZnO powder. The sample, inlet system, and nozzle were heated to 30 °C. Exposures were made with nozzle-to-plate distances of 50 and 25 cm. Optical densities were recorded on a Agfa Duoscan HiD scanner and the data processed as described in ref 27. Atomic scattering factors were taken from ref 28. Experimental backgrounds were drawn as cubic spline functions to the difference between experimental and theoretical molecular intensity curves. Structure refinements were based on data from two plates for each distance. The experimental intensity data extended from 2.0 to 18.0 $Å^{-1}$ and from 8.0 to 35.8 $Å^{-1}$ for the 50 and 25 cm nozzle-to-plate distances, respectively. For both curves an increment of 0.2 $Å^{-1}$ was used. In the overlap region between $s = 8$ and 18 $Å^{-1}$, the data have been combined to a single curve (Figure 2).

Acknowledgment. We thank the Deutsche Forschungsgemeinschaft (DFG) for financial support of the Russian−German Cooperation (413 RUS 113/69). A.V.B. is grateful for a fellowship from the DFG. The CSIC-Udelar and Alexander von Humboldt-Stiftung are acknowledged for partial support for the realization of this project. The contents of this publication do not necessarily reflect the views or policies of the DHHS, nor does mention of trade names, commercial products, or organizations imply endorsement by the U.S. Government.

References and Notes

(1) Samdal, S.; Seip, H. M. *J. Mol. Struct.* **1975**, *28*, 193.
(2) Pyckhout, W.; van Nuffel, P.; van Alsenoy, C.; van den Enden, L.; Geise, H. J. *J. Mol. Struct.* **1983**, *102*, 333.
(3) Fujitake, M.; Hayashi, M. *J. Mol. Struct.* **1985**, *127* 21.
(4) Leibold, C.; Reinemann, S.; Minkwitz, R.; Resnik, P. R.; Oberhammer, H. *J. Org. Chem.* **1997**, *62*, 6160.
(5) Seip, H. M.; Seip, R. *Acta Chem. Scand.* **1973**, *27*, 4024.
(6) Onda, M.; Toda, A.; Mori, S.; Yamaguchi, I. *J. Mol. Struct.* **1986**, *144*, 47.
(7) Tsuzuki, S.; Houjou, H.; Nakagava, Y.; Hiratani, K. *J. Phys. Chem.* A **2000**, *104*, 1332.
(8) Shishkov, I. F.; Geise, H. J.; van Alsenoy, C.; Khristenko, L. V.; Vilkov, L. V.; Senyavian, V. M.; van der Veken, B.; Herrebout, H.; Lokshin, B. V.; Garkusha, O. G. *J. Mol. Struct.* **2001**, *567/568*, 339.
(9) Federsel, D.; Hermann, A.; Christen, D.; Sander, S.; Willner, H.; Oberhammer, H. *J. Mol. Struct.* **2001**, *567/568*, 127.
(10) Giricheva, N. I.; Girichev, G. V.; Levina, J. S.; Oberhammer, H. *J. Mol. Struct.* **2004**, *703*, 55.
(11) Novikov, V. P.; Vilkov, L. V.; Oberhammer, H. *J. Phys. Chem.* A, **2003**, *107*, 908.
(12) Lokshmaiah, B.; Rao, G. R. *J. Raman Spectrosc.* **1989**, *20*, 439.
(13) Schaefer, T.; Laatikainen, R.; Wilaman, T. A.; Peeling, J.; Penner, G. H.; Baleja, J.; Marat, K. *Can. J. Chem.* **1984**, *62*, 1592.
(14) Emsley, J. W.; Lindon, J. C.; Stephenson, D. S. *J. Chem. Soc., Perkin Trans. 2* **1975**, 1794.
(15) Celebre, G.; Longeri, M.; Emsley, J. W. *Appl. Magn. Res.* **1991**, *2*, 611.

(16) Kieninger, M.; Ventura, O. N.; Diercksen, G. H. F. *Chem. Phys. Lett.* In press.

(17) The MP4 method is described in Krishnan, R.; Pople, J. A. *Int. J. Quantum Chem.* **1978**, *14*, 91.

(18) The MP2 method is described: (a) Moller, C.; Plesset, M. S. *Phys. Rev*. **1934**, *46*, 618. (b) Head-Gordon, M.; Pople, J. A.; Frisch, M. J. *Chem. Phys. Lett*. **1988**, *153*, 503. (c) Frisch, M. J.; Head-Gordon, M.; Pople, J. A.; *Chem. Phys. Lett*. **1990**, *166*, 275. (d) Frisch, M. J.; Head-Gordon, M.; Pople, J. A. *Chem. Phys. Lett*. **1990**, *166*, 281. (e) Head-Gordon, M.; Head-Gordon, T. *Chem. Phys. Lett*. **1994**, *220*, 122. (f) Saebo, S.; Almlof, J. **1989**, *154*, 83.

(19) The 6-311++G(3df,2pd) basis set is described: (a) Krishnan, R.; Binkley, J. S.; Seeger, R.; Pople, J. A. *J. Chem. Phys*. **1980**, *72*, 650. (b) Clark, T.; Chandrasekhar, J.; Spitznagel, G. W.; Schleyer, P. v. R. *J. Comput. Chem.* **1983**, *4*, 294. (c) Frisch, M. J.; Pople, J. A.; Binkley, J. S. *J. Chem. Phys*. **1984**, *80*, 3265.

(20) The B3LYP method is described: (a) Becke, A. D.; *J. Chem. Phys*. **1993**, *98*, 5648. (b) Becke, A. D. *Phys. Rev*. A, **1998**, *38*, 3098. (c) Lee, C.; Yang, W.; Parr, R. G. *Phys. Rev*. B **1998**, *37*, 785. Miehlich, B.; Savin, A.; Stoll, H.; Preuss, H. *Chem. Phys. Lett*. **1989**, *157*, 200.

(21) The pc-3 basis set is described: (a) Jensen, F. *J. Chem. Phys*. **2001**, *115*, 9113, **2002**, *116*, 3502(E). (b) Jensen, F. *J. Chem. Phys*. **2002**, *116*, 7372.

(22) Frisch, M. J.; Trucks, G. W.; Schlegel, H. B.; Scuseria, G. E.; Robb, M. A.; Cheeseman, J. R.; Montgomery, J. A., Jr.; Vreven, T.; Kudin, K. N.; Burant, J. C.; Millam, J. M.; Iyengar, S. S.; Tomasi, J.; Barone, V.;. Mennucci, B; Cossi, M.; Scalmani, G.; Rega, N.; Petersson, G. A.; Nakatsuji, H.; Hada, M.; Ehara, M.; Toyota, K.; Fukuda, R.; Hasegawa, J.; Ishida, M.; Nakajima, T.; Honda, Y.; Kitao, O.; Nakai, H.; Klene, M.; Li, X; Knox, J. E.; Hratchian, H. P.; Cross, J. B.; Adamo, C.; Jaramillo, J; Gomperts, R.; Stratmann, R. E.; Yazyev, O.; Austin, A. J.; Cammi, R.; Pomelli, C.; Ochterski, J. W.; Ayala, P. Y.; Morokuma, K.; Voth, G. A.; Salvador, P.; Dannenberg, J. J.; Zakrzewski, V. G.; Dapprich, S.; Daniels, A. D.; Strain, M. C.; Farkas, O.; Malick, D. K.; Rabuck, A. D.; Raghavachari, K.; Foresman, J. B.; Ortiz, J. V.; Cui, Q.; Baboul, A. G.; Clifford, S. Cioslowski, J.; Stefanov, B. B.; Liu, G; Liashenko, A.; Piskorz, P.; Komaromi, I.; Martin, R. L.; Fox, D. J.; Keith, T.; Al-Laham, M. A.; Peng, C. Y.; Nanayakkara, A.; Challacombe, M.; Gill, P. M. W.; Johnson, B.; Chen, W.; Wong, M. W.; Gonzalez, C.; Pople, J. A. *Gaussian 03*, Revision B.04; Gaussian, Inc., Pittsburgh, PA, 2003.

(23) Sipachev, V. A. *J. Mol. Struct. (THEOCHEM)* **1985**, *121*, 143. Sipachev, V. A. In *Advances in Molecular Structure Research;* Hargittai, I., Hargittai, M., Eds.; JAI Press: New York, 1999; Vol. 5, p 263.

(24) Andersen, B.; Seip, H. M.; Strand, T. G.; Stølevik, R. *Acta Chem. Scand*. **1969**, *23*, 3224.

(25) Bastiansen, O.; Kveseth, K.; Møllendal, H. *Top. Curr. Chem*. **1978**, *81*, 99. Ter Brake, J. H. M.; Mijlhof, F. C.; J. Mol. Struct. **1981**, *77*, 109.

(26) Oberhammer, H. *Molecular Structure by Diffraction Methods*; The Chemical Society: London, 1976; Vol. 4, p 24.

(27) Atavin, E. G.; Vilkov, L. V. *Instrum. Exp. Techniques* **2002**, *45*, 27 (in Russian).

(28) Ross, A. W.; Fink, M.; Hilderbrandt. R. L. *International Tables for Crystallography*, Kluwer Academic Publishers: Dordrecht, 1992; C, p245.